Available online at www.sciencedirect.com

ScienceDirect

Journal of the Franklin Institute 360 (2023) 9115–9138

www.elsevier.com/locate/jfranklin

Cascade ADRC with neural network-based ESO for hypersonic vehicle

Lei Liu, Yongxiong Liu, Lilin Zhou, Bo Wang*, Zhongtao Cheng, Huijin Fan

National Key Laboratory of Science and Technology on Multispectral Information Processing, School of Artificial Intelligence and Automation, Huazhong University of Science and Technology, Wuhan, Hubei 430074, China

Received 6 October 2021; received in revised form 22 August 2022; accepted 17 September 2022
Available online 26 September 2022

Abstract

In this paper, active disturbance rejection control (ADRC) based on a neural network has been investigated for the attitude control of the hypersonic vehicle (HV) with uncertain disturbances, which are regarded as a strongly time-varying, nonlinear, and coupled system. The structure of nonlinear state error feedback (NLSEF) with an Extended State Observer (NLSEF+ESO) utilized in ADRC is considered to have good disturbance resistance ability in engineering applications with less dependence on the mathematical model of the system. However, the strong coupling of the HV makes it complicated to separately design ADRC for each channel. In addition, the bandwidth and parameters of the ESO can seriously affect the performance of the ADRC, while jitter occurs when they are not well matched. A cascade active-rejection control scheme is designed by introducing the Radial Basis Function (RBF) Neural Network to substitute the ESO in ADRC, which mitigates the shortcoming of ADRC in addressing the control problems of the MIMO system with coupling disturbances. The NNESO can adapt well to disturbance characteristics through online training and fitting and can effectively reduce the jitter of the control. The stability of the NNESO is proved by Lyapunov stability theory, and the numerical simulations are presented to demonstrate the effectiveness of our theoretical results. In summary, the proposed NNESO-based cascade ADRC is an effective method for solving the problem of HV control with better disturbance resistance.

* Corresponding author.
E-mail address: wb8517@hust.edu.cn (B. Wang).

https://doi.org/10.1016/j.jfranklin.2022.09.019

1. Introduction

Hypersonic flight vehicles comprise a type of highly maneuverable aircraft with a high flight speed and a flight altitude of approximately 20 to 100 km, which is referred to as the near space. The flight speed is often greater than Mach 5, which becomes significant because of its greater advantages in speed and altitude and because it is more suitable for the demand of high-altitude fields and the rapidity of future space vehicles. With the continuous development of science and technology, many countries have invested much in developing hypersonic flight vehicles to occupy an important position in the aerospace field and national defense security. Moreover, this investment can also help grasp the initiative of flying space in the future. Therefore, research on hypersonic flight vehicles is considered one of the hottest research directions in the 21st century [1,2]. This research not only involves multiple frontier subjects but also applies to many frontier technologies in other fields. Therefore, the study of hypersonic flight vehicles is a very complicated system engineering field [3–5].

Research on hypersonic flight vehicles involves many aspects, including materials science, theoretical mathematics, computer science, dynamics, and control science. Among them, the attitude control of hypersonic flight aircraft is an important part to ensure that the aircraft can fly according to the planned trajectory. Because the hypersonic flight vehicle has the inherent characteristics of rapidity, nonlinearity, large disturbance and strong coupling, the attitude control of the hypersonic flight vehicle will be more complicated than other kinds of aircraft [6,7]. Many scholars have proposed many different methods to complete the attitude control of hypersonic flight vehicles. Robust control is a relatively mature method. The advantage of robust control is that it can remain stable in the face of large amounts of disturbance [8,9]. Many methods such as sliding mode variable structure control [10,11], feedback linearization control [12], and backstepping control have been developed in recent years [13,14]. Model-based control methods have been quickly developed in recent decades and have had an essential role in the aerospace field because of their reliability. However, in the hypersonic flight vehicle control problem, there are increasing difficulties in the design of control systems based on accurate models. Thus, model-free control methods, such as active disturbance rejection control (ADRC) [15,16] and neural network control, have developed rapidly in recent years [17,18].

ADRC is a relatively popular control method that has been developed in recent years and that is widely implemented in flight vehicle control [19]. The ADRC method has become popular in practical engineering because it is convenient for controller design, such as the PID method. The addition of an extended observer and nonlinear feedback has greatly improved tracking accuracy and speed. Thus, the application of ADRC in the field of hypersonic flight vehicles has gradually increased in recent years. In [20], a method for controlling hypersonic flight vehicles using ADRC was proposed. By dividing the disturbance into harmful and beneficial parts, an extended observer was employed to compensate for the total disturbance and to eliminate the harmful disturbance. Tian [21] designed a cascaded ADRC for airbreathing hypersonic vehicles. First, feedback linearization (FL) and the equivalent input disturbance (EID) technique are employed to decouple a nonlinear uncertain system into several subsystems in canonical form to simplify the direct design of the ADRC controller for each subsystem. For autopilot design, the ADRC strategy enables precise tracking for velocity and altitude reference commands in the presence of severe parametric perturbations and atmospheric disturbances using only measurable output information. The total concentrated disturbance in the system used an extended observer for observation

and elimination. In this way, the anti-disturbance capability of the system was effectively improved.

Neural networks have become a controversial research topic in recent years and are widely employed in the field of artificial intelligence and control. A neural network is a network structure that can conserve specific information through previous learning. With an increase in the number of requirements for hypersonic aircraft control, neural networks have also been introduced into the control scheme in recent years. In reference [22], considering the state constraints and uncertainties of a system, multiple radial basis function (RBF) neural networks [23] were selected to approximate the uncertainties of the system; the adaptive attitude controller was designed; and a good control effect was achieved. Therefore, a neural network is an efficient way to solve the unknown uncertainties in a system. In [24], fault-tolerant control combined with a neural network was proposed. In consideration of system uncertainties and actuator failures, the neural network was selected to replace the dynamic matrix for boundary estimation to reduce the calculation cost of the entire system and to ensure real-time control.

Although ADRC can provide effective control for hypersonic flight vehicles, several limitations should be considered and improved for the traditional ADRC. First, since ADRC method only considers the control problem of the SISO system, it is inconvenient to be promoted directly to the MIMO system with severe coupling. Second, the control variable of ADRC always has large jitter because of the unsmooth external disturbances.

In this study, an ADRC based on a neural network is proposed to solve the attitude control problem of hypersonic flight vehicles under disturbance. In the ADRC, the disturbance in the system is identified by the extended states and then directly compensated for in the actual control variables. ADRC uses a single variable to identify complicated disturbances of the system and is directly applied to actual control, which might cause greater jitter in the actual control system when the parameters do not match. This approach is obviously not conducive to practical engineering applications. In this paper, neural networks are employed to observe the extended states to identify the system disturbances and compensate, which means that the network structure is selected to replace a single variable. In addition, since the extended states in the ADRC cannot recognize the disturbances between two coupling channels, the active disturbance rejection control can only be designed for a single channel, which makes parameter design difficult. However, the attitude control of hypersonic flight vehicles is a MIMO system. In this paper, a neural network is introduced to directly recognize the disturbance of multiple channels so that we do not have to disregard the coupling among multiple channels to meet the requirements of the ADRC. The proposed method simplifies the controller design. The main contributions of this study are presented as follows:

(1) A novel NNESO is proposed to recognize the disturbances to reduce the jitter of the control. We design a neural network-based extended state observer (NNESO) in the ADRC scheme. The network structure is used to identify the disturbance of the system, which can reduce the jitter of the ADRC because of the inherent anti-jitter abilities of the neural network.
(2) A multichannel coupling, anti-disturbance control method for MIMO systems is provided. The traditional ADRC and ESO are weak in addressing the control problem of the MIMO system with coupling disturbances. The proposed NNESO can directly identify the disturbances of hypersonic flight vehicles, including the couplings among multiple channels. Furthermore, the control accuracy can also be improved through the multichannel coupling controller design compared with the decoupled single channel design methods.

The remainder of this paper is organized as follows: Section 2 introduces the ADRC and neural network and describes the mathematical model of a hypersonic flight vehicle. In Section 3, we design the ADRC controller based on the neural network and then analyze the stability of the extended observer combined with the neural network. Section 4 verifies the effectiveness by numerical simulation. Section 5summarizes the work of this article.

2. Problem formulation and preliminaries

In this section, we describe the mathematical model of hypersonic flight vehicles. The mathematical model of the hypersonic flight vehicle will be processed to facilitate the design of the controller. Since this article proposes an ADRC based on a neural network, a brief introduction to the structure of the neural network used in this article and ADRC will also be given.

2.1. Problem formulation

According to the literature [25], the attitude system of the hypersonic flight vehicle can be described by the following mathematical model:

$$\begin{aligned}
\dot{\alpha} &= -p\cos\alpha\tan\beta + q - r\sin\alpha\tan\beta - \frac{L}{MV\cos\beta} + \frac{g}{V\cos\beta}[\sin\alpha\sin\theta + \cos\alpha\cos\phi\cos\theta] \\
\dot{\beta} &= p\sin\alpha - r\cos\alpha + \frac{Y}{MV} + \frac{g}{V}[\cos\alpha\sin\beta\sin\theta + \cos\beta\cos\theta\sin\phi - \sin\alpha\sin\beta\cos\phi\cos\theta] \\
\dot{\phi} &= p + \tan\theta(q\sin\phi + r\cos\phi)
\end{aligned} \tag{1}$$

$$\begin{aligned}
\dot{p} &= I_2 pq + I_1 qr + I_3 l + I_4 n \\
\dot{q} &= I_5 pr - I_6\left(p^2 - r^2\right) + I_7 m \\
\dot{r} &= -I_2 qr + I_8 pq + I_4 l + I_9 n
\end{aligned} \tag{2}$$

where α, β and ϕ represent the three attitude angles of the aircraft, namely, the angle of attack, side slip angle, and roll angle; p, q and r represent the rotation angular rate of each channel of the aircraft, namely, the roll rate, pitch rate, and yaw rate; and θ, ψ M and V are the pitch angle, yaw angle, mass of the hypersonic flight vehicle and speed of the aircraft. The values of θ, ψ and V can be calculated by the following equations:

$$\begin{aligned}
\dot{V} &= -\frac{D}{M} + g(\cos\beta\sin\alpha\cos\phi\cos\theta + \sin\beta\cos\theta\sin\phi - \cos\alpha\cos\beta\sin\theta) \\
\dot{\theta} &= \cos\phi q - \sin\phi r \\
\dot{\psi} &= \frac{\sin\phi q + \cos\phi r}{\cos\theta}
\end{aligned} \tag{3}$$

For I_j, $j = 1, 2, ..., 9$ in (2), the specific form can refer to formula (4)

$$\begin{aligned}
&I_1 = -\frac{I_z(I_z - I_y) + I_{xz}^2}{I_x I_z - I_{xz}^2},\ I_2 = \frac{I_{xz}(I_x - I_y + I_z)}{I_x I_z - I_{xz}^2},\ I_3 = \frac{I_z}{I_x I_z - I_{xz}^2},\ I_4 = \frac{I_{xz}}{I_x I_z - I_{xz}^2} \\
&I_5 = \frac{I_z - I_x}{I_y},\ I_6 = \frac{I_{xz}}{I_y},\ I_5 = \frac{1}{I_y},\ I_8 = \frac{I_x(I_x - I_y) + I_{xz}^2}{I_x I_z - I_{xz}^2},\ I_9 = \frac{I_x}{I_x I_z - I_{xz}^2}
\end{aligned} \tag{4}$$

where I_x, I_y and I_z refer to the moment of inertia of each channel of the aircraft and I_{xz} is the product of inertia.

In (1), (2) and (3), D, L and Y represent the aerodynamic force, and l, m and n represent the aerodynamic moment. The aerodynamic force and aerodynamic moment are mainly related

to the attitude angle, speed and rudder angle of the aircraft. The relationship between them can be expressed by the following equations:

$$\begin{aligned} D &= \bar{q}S\left(C_D(\alpha,V)+C_{D\delta_e}(\alpha,V)\delta_e+C_{D\delta_a}(\alpha,V)\delta_a+C_{D\delta_r}(\alpha,V)\delta_r\right)\\ L &= \bar{q}S\left(C_L(\alpha,V)+C_{L\delta_e}(\alpha,V)\delta_e+C_{L\delta_a}(\alpha,V)\delta_a\right)\\ Y &= \bar{q}S\left(C_L(\alpha,\beta,V)+C_{Y\delta_e}(\alpha,V)\delta_e+C_{Y\delta_a}(\alpha,V)\delta_a+C_{Y\delta_r}(\alpha,V)\delta_r\right) \end{aligned} \tag{5}$$

$$\begin{aligned} l &= \bar{q}bS_{ref}\left(C_l(\alpha,\beta,V)+C_{lp}(\alpha,V)\tfrac{pb}{2V}+C_{lr}(\alpha,V)\tfrac{rb}{2V}+C_{l\delta_e}(\alpha,V)\delta_e+C_{l\delta_a}(\alpha,V)\delta_a+C_{l\delta_r}(\alpha,V)\delta_r\right)\\ m &= \bar{q}cS_{ref}\left(C_m(\alpha,V)+C_{mq}(\alpha,V)\tfrac{qc}{2V}+C_{m\delta_e}(\alpha,V)\delta_e+C_{m\delta_a}(\alpha,V)\delta_a+C_lm(\alpha,V)\delta_r\right)\\ n &= \bar{q}bS_{ref}\left(C_n(\alpha,\beta,V)+C_{np}(\alpha,V)\tfrac{pb}{2V}+C_{nr}(\alpha,V)\tfrac{rb}{2V}+C_{n\delta_e}(\alpha,V)\delta_e+C_{n\delta_a}(\alpha,V)\delta_a+C_{n\delta_r}(\alpha,V)\delta_r\right) \end{aligned} \tag{6}$$

where b, S_{ref}, c and $\bar{q}$ are the lateral-directional reference length, reference area of the aircraft, longitudinal reference length and dynamic pressure, respectively. δ_a, δ_e and δ_r represent the rudder of the aircraft, which are the right elevon, left elevon, and rudder, respectively. The control amount of the rudder of the aircraft to the control object is expressed by Substituting Eqs. (5) and (6) into Eqs. (1) and (2) To adapt to the design of the ADRC, we will reorganize the equations as follows:

$$\begin{aligned} \dot{x}_1 &= F_1(x_1,x_3,V)+g_1(x_1)x_2\\ \dot{x}_2 &= F_2(x_1,x_2,V)+g_2(x_1,V)u\\ \dot{x}_3 &= f_3(\theta,\psi)x_2 \end{aligned} \tag{7}$$

where $x_1=[\alpha,\beta,\phi]^T$, $x_2=[p,q,r]^T$, $u=[\delta_a,\delta_e,\delta_r]^T$ and $x_3=[\theta,\psi]^T$. Eq. (7) defines the control objects of this article. Specifically, the third equation of (7) does not define the direct control object of this paper, but the state is needed in the design process of the controller. $F_i(\cdot)(i=1,2)$ represents the disturbance of the system, including the internal disturbance and external disturbance of the system.

Lemma 1 [26]: For bounded initial status, if there exists a continuous and positive-definite Lyapunov function $V(x)$ satisfying $\pi_1(\|x\|)\le V(x)\le\pi_2(\|x\|)$, such that $\dot{V}(x)\le-\kappa V(x)+c$, where $\pi_1,\pi_2:R^n\to R$ are class K functions and c is a positive constant, then the solution $x(t)$ is uniformly bounded.

2.2. Preliminary

In this paper, we propose a novel ADRC structure with a neural network state observer. The neural network is mainly employed to replace the original extended state observer (ESO) in the ADRC. Therefore, the neural network can learn all disturbances of the system through learning and compensates in the control. Particularly, to guarantee the real-time performance of the controller, high-speed learning ability is required in the neural network design. Therefore, the RBF neural network is preferred here to construct the novel NNESO.

2.2.1. RBF neural network structure analysis

The RBF neural network can be described as follows:

$$y=W^T\vec{\sigma}(\hat{x}) \tag{8}$$

where $W=[\omega_1\omega_2\cdots\omega_{N_3}]\in R^{(N_2+1)\times N_3}$, $\omega_i\in R^{N_2+1}$ is the weighing matrix of the RBF and $\hat{x}=[1x_1x_2\cdots x_{N_1}]^T\in R^{N_1+1}$, $\vec{\sigma}(z)=[1,\sigma(z_1),\sigma(z_2),\cdots,\sigma(z_{N_2})]^T$, $\sigma(z)=\exp(-\frac{\|\hat{x}-r_i\|^2}{2\varphi_i^2})$ where $r_i\in R^{N_1+1}$ is the center vector and φ_i is the width of the ith neuron.

Analyzing the structure of the RBF neural network, because of the maintenance of the nonlinear characteristics, we need to complete the learning of the linear layer weights from the hidden layer to the output layer only [27]. In addition, the RBF neural network has the ability to approximate any nonlinear function [28]. Thus, for any nonlinear function Π, there is an ideal RBF neural network that makes Eq. (9) true.

$$\Pi = W^T \vec{\sigma}(\hat{x}) + \varepsilon(\hat{x}) \tag{9}$$

where $\varepsilon(\hat{x})$ represents the approximating error of the neural network. The error between the ideal weight W and the estimated weight $\hat{W}$ can be defined as $\tilde{W} = \hat{W} - W$.

2.2.2. ADRC principle

The ADRC controller is mainly composed of three parts: tracking differentiator (TD), extended state observer (ESO), and nonlinear state error feedback (NLSEF) [29]. Eq. (10) uses a second-order system as an example to give a brief description of these three parts. For a second-order system:

$$\begin{cases} \dot{x}_1 = x_2 \\ \dot{x}_2 = f(x_1, x_2) + bu \\ y = x_1 \end{cases} \tag{10}$$

where $f(x_1, x_2)$ represents the disturbance of the system, including the internal disturbance and external disturbance of the system. tracking differentiator (TD)

$$\begin{aligned} e_1 &= v_1 - x_d \\ \dot{v}_1 &= v_2 \\ \dot{v}_2 &= -fhan(e_1, v_1, r, h) \end{aligned} \tag{11}$$

where x_d represents the desired attitude angles of the HV system, r is the control parameter, and h is the simulation step size. $fhan(\cdot)$ specific form can refer to the literature [29] as follows:

$$\begin{cases} d = rh^2 \\ a_0 = hx_2 \\ y = x_1 + a_0 \\ a_1 = \sqrt{d(d + 8|y|)} \\ a_2 = a_0 + sign(y)(a_1 - d)/2 \\ a = (a_0 + y)fsg(y, d) + a_2(1 - fsg(a, d)) \\ fsg(x, d) = (sign(x + d) - sign(x - d))/2 \\ fhan = -r\left(\frac{a}{d}\right)fsg(a, d) - r \cdot sign(a)(1 - fsg(a, d)) \end{cases} \tag{12}$$

extended state observer (ESO)

$$\begin{cases} e = z_1 - y \\ fe = fal(e, \alpha_1, \delta) \\ fe_1 = fal(e, \alpha_2, \delta) \\ \dot{z}_1 = z_2 - \beta_{o1} e \\ \dot{z}_2 = z_3 - \beta_{o2} fe + bu \\ \dot{z}_3 = -\beta_{o3} fe_1 \end{cases} \tag{13}$$

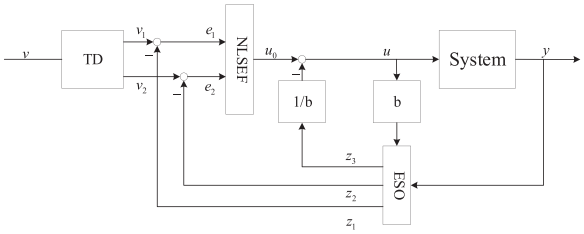

Fig. 1. Structure diagram of the ADRC.

where β_{o1}, β_{o2} and β_{o3} are the control parameters of the ESO. The expression of $fal(\cdot)$ can refer to the literature [29] as follows:

$$fal(e,\alpha,\delta)=\begin{cases}\frac{e}{\delta^{1-\alpha}}, & |e|\le\delta\\ |e|^{\alpha}sign(e), & |e|>\delta\end{cases} \tag{14}$$

where α and δ are the parameters that we aim to design, which need to satisfy the inequalities $0<\alpha<1$ and $\delta>0$.

Nonlinear state error feedback (NLSEF)

There are many forms of nonlinear state error feedback. For different systems, the form of nonlinear state error feedback may also differ. The two most common forms are presented as follows:

$$u_0=\beta_1 fal(e_1,\alpha_1,\delta)+\beta_2 fal(e_2,\alpha_2,\delta) \tag{15}$$

or

$$u_0=fhan(e_1,c\cdot e_2,r,h_1) \tag{16}$$

where e_1 and e_2 represent the error between the TD and the ESO.

The structure diagram of the ADRC is shown below: Fig. 1.

3. NN based ADRC design

3.1. Controller's structure

ADRC is considered to have good disturbance resistance ability in engineering applications with less dependence on the mathematical model of the system, based on its "NLSEF+ESO" structure. By using ESO, we can estimate not only each state variable but also the model uncertainties and external disturbances. However, the bandwidth and parameters of ESO can seriously affect the performance of the ADRC, while jitter occurs when they do not match the disturbance characteristics. On the other hand, the strong coupling of the three channels is an inherent characteristic of the HV. It is complicated to separately design ADRC and ESO for each channel. In this situation, coupling is always regarded as an external disturbance by using the traditional ADRC; it will increase the complexity of the controller and increase the burden of the controller.

Owing to the abovementioned reasons, we design a novel, cascade dual closed-loop ADRC for model (7). Here, inner loop and outer loop controllers will be designed separately with a neural network. The outer loop will be responsible for tracking the desired attitudes of

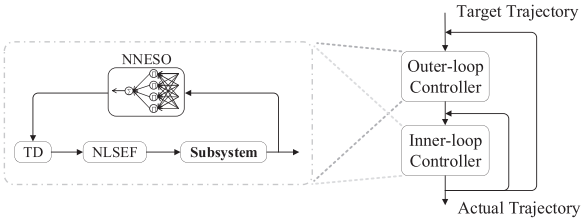

Fig. 2. General framework diagram of the proposed algorithm.

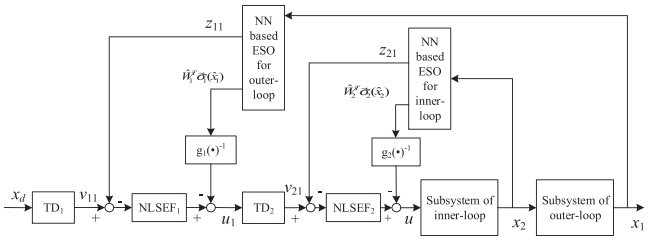

Fig. 3. Structure diagram of ADRC based on NN.

the entire system and for generating the desired attitudes for the inner loop. The inner loop mainly tracks the angular rate commands generated by the outer loop. Simultaneously, neural networks are separately introduced into the control of the inner and outer loops. The general framework is intuitively described in Fig. 2.

After introducing the neural network in the ADRC framework, the disturbances of the inner-loop and outer-loop subsystems can be estimated by the neural network. In this way, a new NN-based ESO is constructed. The structure diagram of ADRC based on a neural network is given in Fig. 3.

3.1.1. ADRC design of the outer loop subsystem

For the controller design of the outer loop, the control object is the subsystem in the first equation of Eq. (7).

$$\dot{x}_1 = F_1(x_1, x_3, V) + g_1(x_1)x_2 \tag{17}$$

Here, the state x_2 is designed as an equivalent control of the outer loop subsystem. To improve the control performance, we design an ADRC with TD, ESO and NLSEF.

TD design for the outer loop

The control object (17) of the outer loop subsystem can be identified as a first-order MIMO system. In ADRC, the TD can simultaneously obtain the desired command and its derivative. However, for the first-order out loop subsystem (17), we cannot directly use the derivative of the desired command. Nevertheless, the transition process can still be designed here using the TD, without the differential signal output in control. The TD for the outer loop controller is designed as shown in Eq. (18):

$$\begin{aligned} e_1 &= v_{11} - x_d \\ \dot{v}_{11} &= v_{12} \\ \dot{v}_{12} &= -fhan(e_1, v_{12}, r, h) \end{aligned} \tag{18}$$

where v_{11}, v_{12} represent the signal and differential of the output of the TD, $x_d=[\alpha_d, \beta_d, \phi_d]^T$ represents the expected attitudes of the aircraft given by the guidance law, and h represents the simulation step.

Neural Network-based ESO (NNESO) design

The main purpose of the ESO is to observe the extended states and to approximate the disturbances of the system. The ADRC can then compensate for the control by the identified disturbances to enhance the disturbance suppression ability. However, in the ADRC controller design, the original ESO is always utilized to observe a certain extended state to identify external disturbances. Therefore, in this traditional ADRC structure, heavy jitter is always unavoidable in the controller if the disturbances are coupled in multiple control channels, such as the attitude control system of the HV.

In this paper, a neural network is introduced in ADRC to replace the traditional ESO, namely, the NN-based ESO, which can effectively reduce the jitter. Thus, the coupling disturbance between two different channels can be identified through the nonlinear network structure of the NN. Therefore, the NN allows us to solve the attitude control problem of the hypersonic flight vehicle, which is a typical MIMO system. For the outer loop system (17), the NNESO can be designed as shown in Eq. (19).

$$\begin{aligned} e_1 &= z_{11} - x_1 \\ fe_1 &= fal(e_1, \alpha_1, \delta_1) \\ \dot{z}_{11} &= \hat{W}_1^T \vec{\sigma}_1(\hat{x}_1) - \beta_1 \cdot e_1 + g_1(\cdot) \cdot u_1 \\ \dot{\hat{W}}_1 &= \Lambda_1 \left(-\vec{\sigma}_1(\hat{x}_1) fe_1^T - K_{W_1} \hat{W}_1 \right) \end{aligned} \tag{19}$$

where u_1 represents the virtual control of the outer loop subsystem (17), which is the desired attitude of the inner loop subsystem, rather than the actual control of the system (7). Therefore, the virtual control u_1 is the desired command x_2 of the inner loop subsystem. z_{11} is the observed state corresponding to the original system x_1. $\hat{W}_1^T \vec{\sigma}_1(\hat{x}_1)$ is the estimated value of $F_1(x_1, x_3, V)$ through the neural network, $\hat{x}_1 = [x_1^T x_3^T V]^T$, and $\beta_1=\beta_1^T>0$. Λ_1 and K_{W_1} are the designed parameters of the update law of the neural network.

NLSEF for the outer loop subsystem

According to the designed NNESO, the NLSEF for the outer loop is designed as shown in Eq. (20) to construct the virtual control u_1.

$$\begin{aligned} es_1 &= v_{11} - z_{11} \\ u_1 &= k_1 fal(es_1, r_1, h) - g_1(\cdot)^{-1} \left(\hat{W}_1^T \vec{\sigma}_1(\hat{x}_1) \right) \end{aligned} \tag{20}$$

3.1.2. ADRC design of the inner loop subsystem

For the controller design of the inner loop subsystem, the control object is presented as the second equation of Eq. (7).

$$\dot{x}_2 = F_2(x_1, x_2, V) + g_2(x_1, V)u \tag{21}$$

The controller design process of the inner-loop subsystem is similar to that of the outer-loop subsystem. Referring to the TD, ESO and NLSEF design of the outer loop subsystem, we can obtain those of the inner subsystem as shown below.

TD

$$\begin{aligned} e_2 &= v_{21} - u_1 \\ \dot{v}_{21} &= v_{22} \\ \dot{v}_{22} &= -fhan(e_2, v_{22}, r, h) \end{aligned} \tag{22}$$

where v_{21} and v_{22} represent the signal and differential, respectively, of the output of the TD. u_1 is the output of the outer loop controller, that is, the desired attitudes of the inner-loop subsystem.

NNESO

$$\begin{aligned} e_2 &= z_{21} - x_2 \\ fe_2 &= fal(e_2, \alpha_2, \delta_2) \\ \dot{z}_{21} &= \hat{W}_2^T \vec{\sigma}_2(\hat{x}_2) - \beta_2 \cdot e_2 + g_2(\cdot) \cdot u \\ \dot{\hat{W}}_2 &= \Lambda_2\left(-\vec{\sigma}_2(\hat{x}_2) fe_2^T - K_{W_2}\hat{W}_2\right) \end{aligned} \tag{23}$$

where u represents the actual control of the inner loop subsystem, which is also the control law of the system's controller. z_{21} is the observed state corresponding to the original system x_2. $\hat{W}_2^T \vec{\sigma}_2(\hat{x}_2)$ is the estimated value of $F_2(x_1, x_2, V)$ by the neural network, where $\hat{x}_2 = [x_1^T x_2^T V]^T$ and $\beta_2 = \beta_2^T > 0$. $\Lambda_2 = 10$ and $K_{W_2} = 0.001$ are the design parameters of the update law of the neural network.

NLSEF

The NLSEF selected for the inner loop subsystem is expressed by Eq. (24):

$$\begin{aligned} es_2 &= v_{21} - z_{21} \\ u &= k_2 fal(es_2, r_2, h) - g_2(\cdot)^{-1}\left(\hat{W}_2^T \vec{\sigma}_2(\hat{x}_2)\right) \end{aligned} \tag{24}$$

3.2. Stability analysis of NNESO

The stability of the ADRC mainly depends on the stability of the ESO. Therefore, it is necessary to analyze the stability of the proposed NNESO. In the above inner loop and outer loop controllers, both NNESOs have similar structures. Here, we only prove the stability of the NNESO of the inner loop subsystem, for example. The inner loop subsystem and the corresponding NNESO are shown in Eqs. (25) and (26).

$$\dot{x}_2 = F_2(x_1, x_2, V) + g_2(x_1, V)u \tag{25}$$

$$\begin{aligned} e_2 &= z_{21} - x_2 \\ fe_2 &= fal(e_2, \alpha_2, \delta_2) \\ \dot{z}_{21} &= \hat{W}_2^T \vec{\sigma}_2(\hat{x}_2) - \beta_2 \cdot e_2 + g_2(\cdot) \cdot u \\ \dot{\hat{W}}_2 &= \Lambda_2\left(-\vec{\sigma}_2(\hat{x}_2) fe_2^T - K_{W_2}\hat{W}_2\right) \end{aligned} \tag{26}$$

For the inner loop subsystem (25), because the neural network has the ability to fit an arbitrary nonlinear function, we assume that there is an ideal neural network that can fit the disturbance:

$$F_2(x_1, x_2, V) = W_2^T \vec{\sigma}_2(\hat{x}_2) \tag{27}$$

Subsystem (25) can be rewritten as:

$$\dot{x}_2 = W_2^T \vec{\sigma}_2(\hat{x}_2) + g_2(x_1, V)u \tag{28}$$

Subsequently, the convergence of the error $e_2 = z_{21} - x_2$ between observer state z_{21} and system state x_2 and the weight error $\tilde{W}_2 = \hat{W}_2 - W_2$ of the neural network can be defined. Based on these definitions, a Lyapunov function can be designed as shown in Eq. (29):

$$V = \frac{1}{2} tr\left(\tilde{W}_2^T \Lambda_2^{-1} \tilde{W}_2\right) + \int_0^{e_2} f e_2 d e_2 \tag{29}$$

Deriving formula (29), we have:

$$\begin{aligned} \dot{V} &= tr\left(\tilde{W}_2^T \Lambda_2^{-1} \dot{\hat{W}}_2\right) + f e_2 \dot{e}_2 \\ &= -tr\left(\tilde{W}_2^T \vec{\sigma}_2(\hat{x}_2) f e_2^T\right) - tr\left(\tilde{W}_2^T K_{W_2} \hat{W}_2\right) \\ &\quad + f e_2^T \left(\hat{W}_2^T \vec{\sigma}_2(\hat{x}_2) - \beta_2 \cdot e_2 - W_2^T \vec{\sigma}_2(\hat{x}_2)\right) \end{aligned} \tag{30}$$

Combining the following two formulas:

$$\begin{aligned} &tr\left(\tilde{W}_2^T \vec{\sigma}_2(\hat{x}_2) f e_2^T\right) = tr\left(f e_2^T \tilde{W}_2^T \vec{\sigma}_2(\hat{x}_2)\right) \\ &= f e_2^T \tilde{W}_2^T \vec{\sigma}_2(\hat{x}_2) \end{aligned} \tag{31}$$

$$\begin{aligned} &2tr\left(\tilde{W}_2^T \hat{W}_2\right) = \left\|\tilde{W}_2\right\|^2 + \left\|\hat{W}_2\right\|^2 - \|W_2\|^2 \\ &\geq \left\|\tilde{W}_2\right\|^2 - \|W_2\|^2 \end{aligned} \tag{32}$$

We have:

$$\begin{aligned} &\dot{V} = tr\left(\tilde{W}_2^T \Lambda_2^{-1} \dot{\hat{W}}_2\right) + f e_2 \dot{e}_2 \\ &\leq -tr\left(\tilde{W}_2^T \vec{\sigma}_2(\hat{x}_2) f e_2^T\right) - \tfrac{K_{W_2}}{2} \left\|\tilde{W}_2\right\|^2 + \tfrac{K_{W_2}}{2} \|W_2\|^2 \\ &+ f e_2^T \tilde{W}_2^T \vec{\sigma}_2(\hat{x}_2) - \beta_2 f e_2^T e_2 \\ &= -\beta_2 f e_2^T e_2 - \tfrac{K_{W_2}}{2} \left\|\tilde{W}_2\right\|^2 + \tfrac{K_{W_2}}{2} \|W_2\|^2 \end{aligned} \tag{33}$$

In the above formula, both $\beta_2 f e_2^T e_2$ and $\frac{K_{W_2}}{2} \|\tilde{W}_2\|^2$ are greater than zero. Therefore, the ESO system can eventually converge to a certain zero domain, and the size of the zero domain can be controlled by adjusting parameter K_{W_2}

4. Simulation and analysis

As previously mentioned, the stability of the ESO combined with the neural network proposed in this paper has been analyzed by Lyapunov stability theory, which will determine the performance of the observer and the entire ADRC system. In this section, the performance of the proposed HV control law will be evaluated by numerical simulation. Two different scenarios are considered in the numerical simulation. In the first scenario, we compare the proposed algorithm with the existing ADRC method to solve the problem of large model deviation. The second scenario demonstrates that the HV trajectory attitude in the actual scene is simulated to verify the practicability and effectiveness of the algorithm.

4.1. Object parameters and simulation environment

First, we give the following parameters related to the experimental environment and HV system: reentry mass of aircraft body $M = 64500$ kg, fuselage length $L = 60.96$ m, wingspan length $b = 18.288$ m, wing reference area $S = 334.73$ m^2, average aerodynamic chord length $c = 24.384$ m, and the distance between pressure center and mass center $x_{cg} = 4.4668$ m. The simulation step $h = 0.01$s. The parameters of the proposed method are set as follows: the designed parameters of the update law of the neural network are taken as $\Lambda_1 = \Lambda_2 = 10$ and $K_{W_1} = K_{W_2} = 0.001$, and the designed parameters of ADRC are selected as $\alpha_1 = \alpha_2 = 0.5$, $\delta_1 = \delta_2 = 0.01$ and $r = 0.5$. In order to obtain the optimized network parameters, we use intelligent optimization algorithm, such as the Differential Evolution (DE) Algorithm with high optimization efficiency, to obtain the initial values of a set of parameters through iterative optimization. Then, based on this set of initial values, some parameters are fine-tuned to get better results.

Second, an RBF neural network is designed and trained online. Only one hidden layer is contained in the inner and outer neural networks. The neural network can ensure the approximation performance and real-time performance because of the simplicity of the RBF structure. The real-time training framework is described as follows: First, a nonlinear mapping $\vec{\sigma}(\hat{x})$ is adopted between the input layer and the hidden layer in Eq. (8). Second, the updating rate of neural network weights is adjusted according to Eqs. (19) and (23). The weight matrix from the hidden layer to the output layer is modified according to the update rate. Considering the approximation capability and rapidity requirements, the number of neurons in the inner layer and outer hidden layer is set to 128 and 64, respectively. As thus, we design a 128-64-1 RBF network, which can adapt to the different approximating tasks of the inner and outer loops of neural networks and avoid the over-fitting problem caused by the large scale of neuron network.

We test the computational cost for the abovementioned method by running the program in MATLAB R2021a. Setting the number of test loops to 50, the computational cost of the learning control is 0.4945 s.

4.2. Simulation with large deviations of model

To demonstrate the advantages of the control method proposed in this paper, we compare the ADRC in [30] with our control method. In the numerical simulation, the mathematical model of the hypersonic flight vehicle that we selected is the Winged-Cone model published by NASA Research Center. The complete structural parameters of this model are provided in Ref. [31]. The functional relationship between the aerodynamic force (moment) and the states of the model is provided in [32].

First, we design the expected attitudes in the following forms:

$$\alpha_{ref} = \begin{cases} -20t \in [0, 20) \\ -20t \in [20, 40) \\ 5t \in [40, 80) \end{cases}, \phi_{ref} = \begin{cases} 0t \in [0, 30) \\ 30t \notin [30, 50) \\ -30t \notin [50, 80) \end{cases}, \beta_{ref} = 0 \tag{34}$$

For the perturbation of the system, the internal and external perturbations of the system can be uniformly compensated by the neural network. Therefore, here, we consider introducing the system's disturbances through the aerodynamic parameters, resulting in additional deviation (40%) for nominal aerodynamic parameters.

The main control parameters for the control method proposed above are designed as follows:

(1) TDs of the inner and outer loop subsystems are designed with the parameters $r_1 = r_2 = diag\{3, 3, 3\}$
(2) NNESOs are designed with the parameters $\beta_1 = diag\{0.2, 0.01, 0.6\}$, $\beta_2 = diag\{200, 0.1, 1\}$, $\Lambda_1 = diag\{0.3, 100, 0.1\}$, $\Lambda_2 = diag\{0.3, 9, 0.01\}$, $K_{W_1} = diag\{0.1, 0.1, 0.1\}$ and $K_{W_2} = diag\{0.01, 0.01, 0.01\}$.
(3) NLSEFs are designed with the parameters $k_1 = diag\{0.2, 0.01, 0.6\}$ and $k_1 = diag\{20, 0.1, 10\}$.

To compare the control effect of the method presented in this paper with that in [30], we give a comparison figure of the attitude angle tracking, the angular rates in each channel of HV attitude control, and the control variable of both control methods, referring to 0, 0 and 0. Subgraph (a) shows the simulation results proposed in this paper, and subgraph (b) shows the simulation results by the method in [30].

Fig. 4 shows that both our method and the method in [30] achieve a good tracking effect for the step instruction in the pitch and rolling channels. In the yaw channel, the yaw angle β can be stabilized at approximately 0. Specifically, the overshoot at approximately 54 seconds by ADRC in [30] can be suppressed well in the rolling channel by using our method. Thus, our method can improve the dynamic performance of the controller.

Furthermore, the advantages of our method can be demonstrated intuitively in Figs. 5 and 6, which show the curves of the angular rate and rudder angle in each channel. Notably, the rudder angles obtained by using our method are smoother than those obtained by the ADRC method in [30]. The attitude angle rate curves in Fig. 5 also presents a similar phenomenon. Therefore, the method proposed in this paper has less jitter and a better control performance.

Nevertheless, because the proposed control method resists the disturbance of the system through the network structure of the RBF neural network, it can achieve smoother tracking effects for rapidly changed disturbances, which is conducive to control jitter reduction. On the other hand, it is difficult to analyze the performance of NNESO to identify disturbances, which are added through the aerodynamic perturbances, because of the unknown specific form of the NN. In Fig. 7, we present the output of the NN of the inner and outer loop subsystems to show the estimation process of the disturbances that concurrently exist in different channels. It follows that the NNESO has an observation effect in the multichannel coupling system.

4.3. Simulation with the coupling effect on the HV system

To verify the superiority of the proposed NNESO-based ADRC method to address the control problems for a multichannel coupled system such as the HV, we compare the disturbance rejection effects in the other two channels when we give sudden steps in the roll channel. The simulation results are shown in Fig. 8.

In Fig. 8(a), the control effect of the proposed method in the roll channel is apparently better than that of the traditional ADRC when we generate a sudden step in the roll channel. Moreover, in the yaw channel, the perturbations due to the coupling are more serious by the traditional ADRC method than by using the proposed method. The reason is that ADRC adopts a single-channel design method, but our method applies a neural network to simultaneously observe disturbances in multiple channels and to carry out an anti-disturbance design

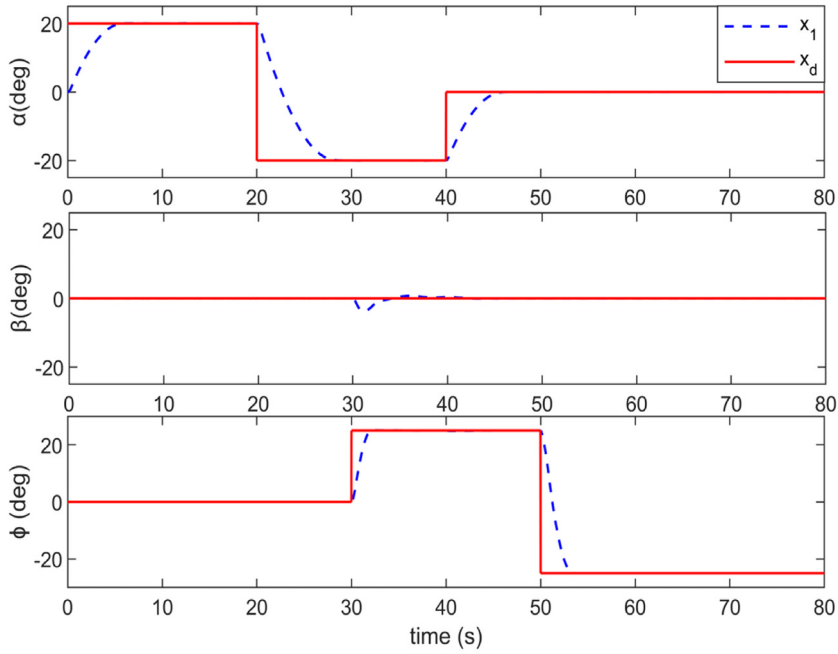

(a) by the proposed method

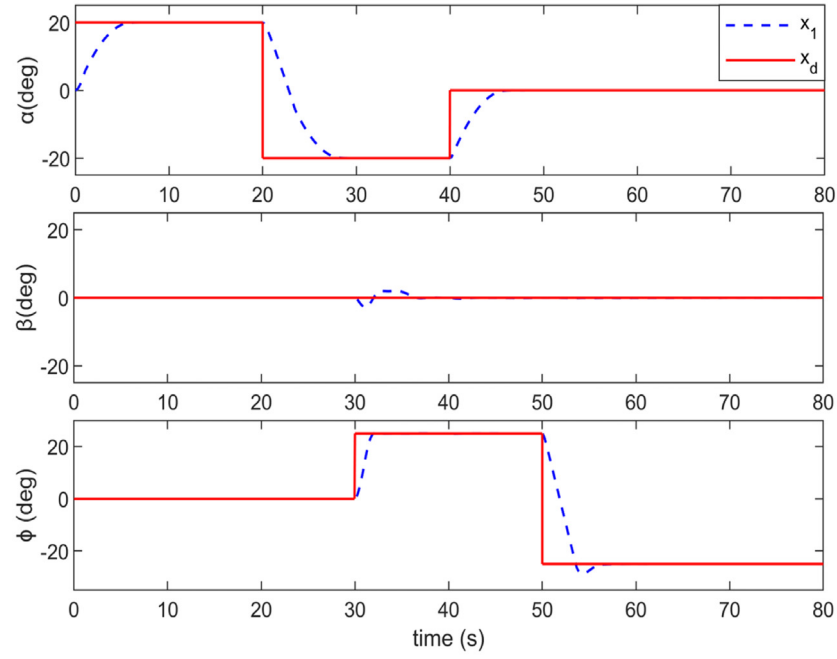

(b) by the method in [30]

Fig. 4. Attitude angle response.

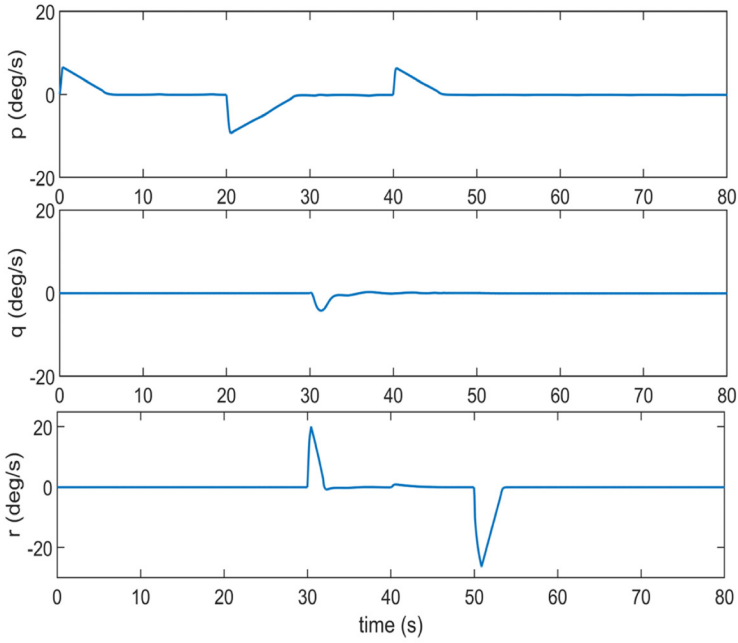

(a) by the proposed method

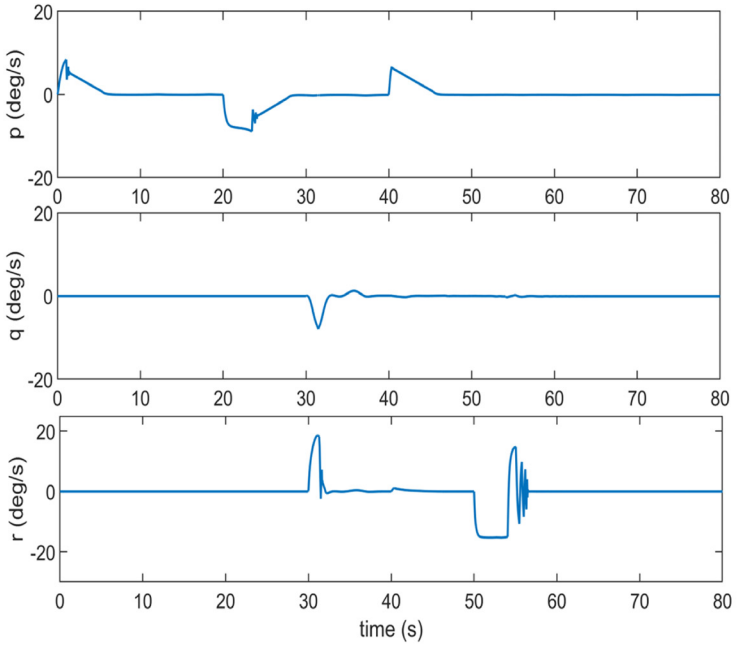

(b) by the method in [30]

Fig. 5. Angular rates.

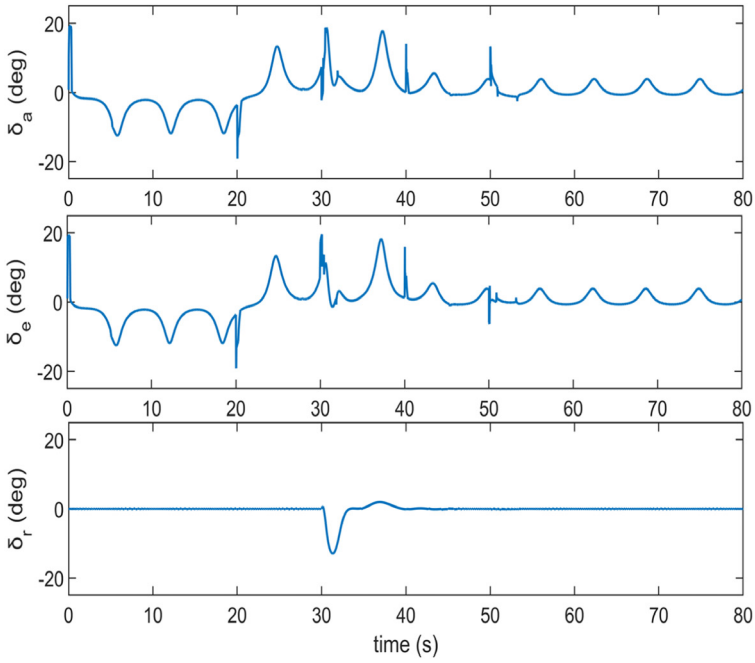

(a) by the proposed method

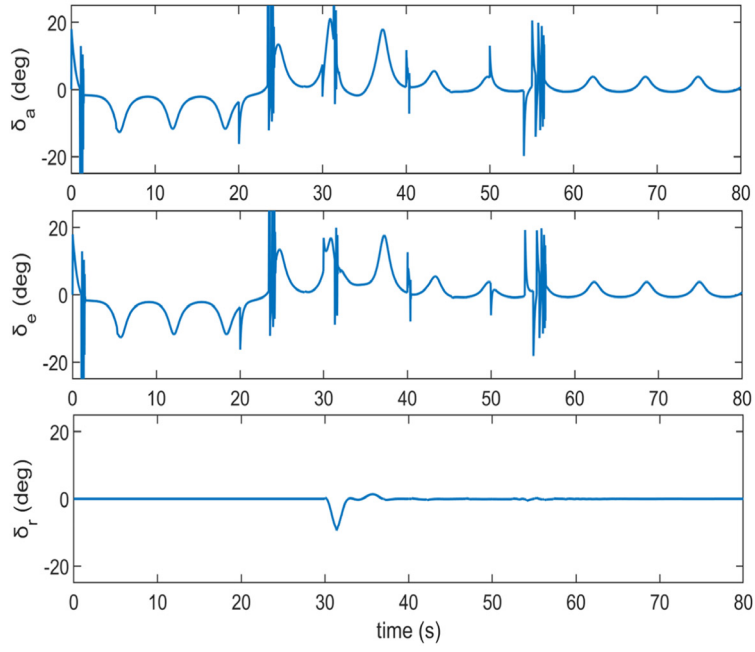

(b) by the method in [30]

Fig. 6. Rudder angles.

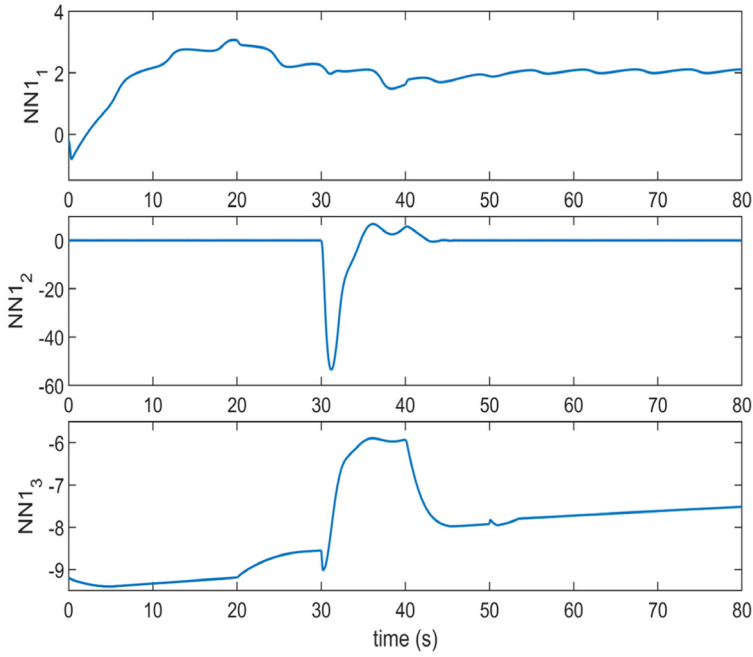

(a) NN output of the outer loop subsystem

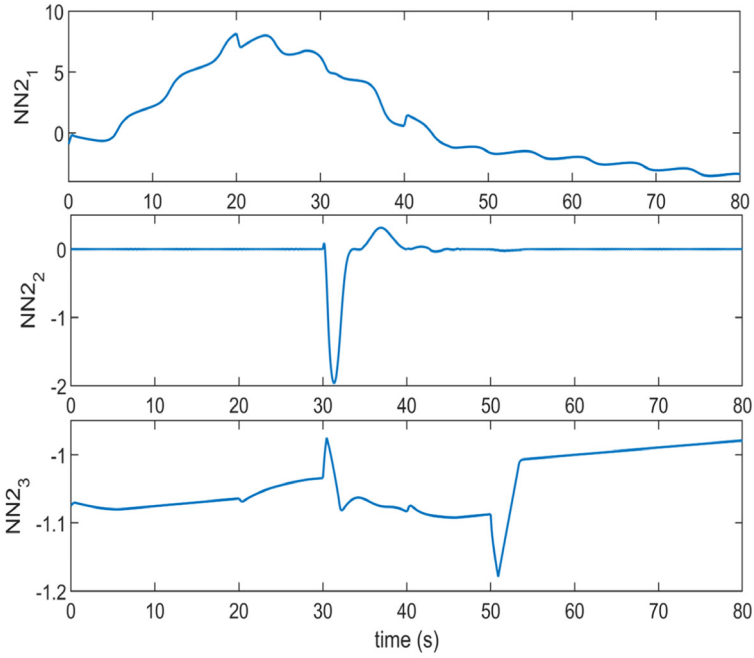

(b) NN output of the inner loop subsystem

Fig. 7. Output of the neural network.

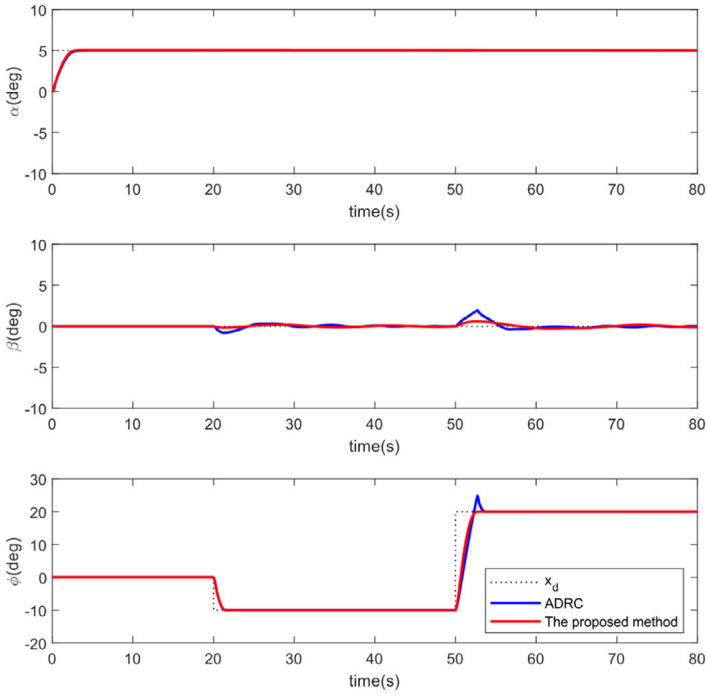

(a) Comparison of the attitude angles

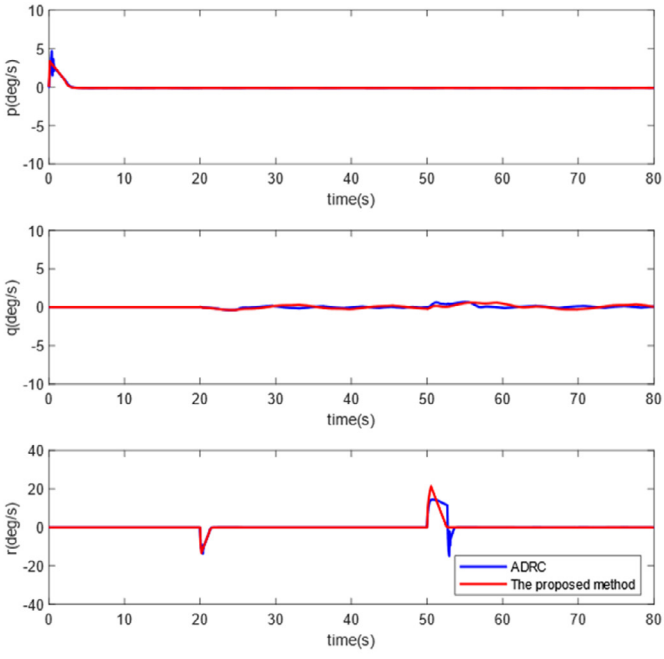

(b) Comparison of the angle velocities

Fig. 8. Comparison of the proposed method and traditional ADRC.

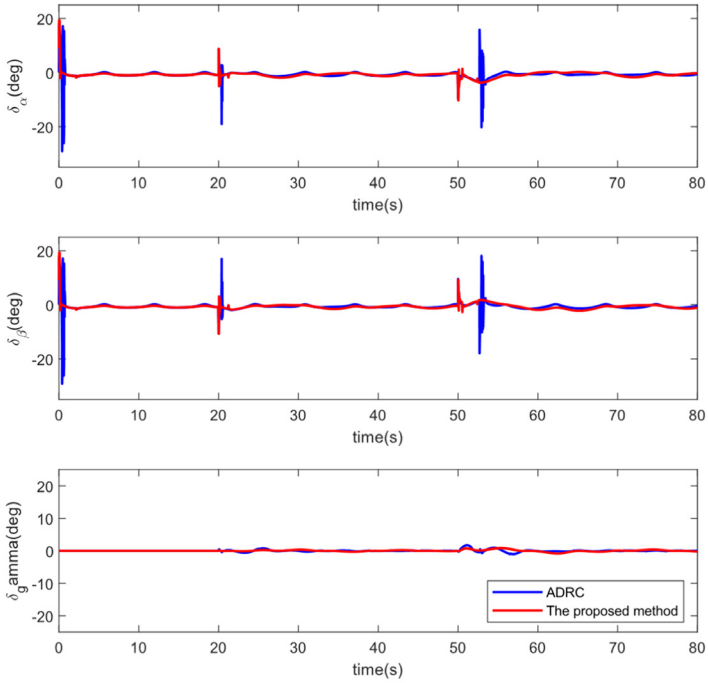

(c) Comparison of the rudder deflections

Fig. 8. Continued

Table 1
Comparison of different control methods in the HV system.

Control method	Key Findings	Corresponding Simulation Results
Proposed Method with NNESO vs. Traditional ADRC	Better attitude tracking performance, especially in the roll channel	Fig. 4(a) and (b)
	Has less jitter and better control performance	Figs. 5(a), (b) and 6(a), (b)
	Has better tracking performance under the influence of coupling interference	Fig. 8(a–c)

for multiple channels. Similar results can be obtained in Fig. 8(b), which shows the angular velocity tracking curves. As shown in Fig. 8(c), the controller jitter on the rudder deflections of the proposed method is greatly improved compared with the traditional ADRC. The improvement by NNESO can effectively reduce the impact of coupling of the HV system on the control performance and can achieve a better control effect.

We can summarize the key findings of the simulation comparisons in Table 1.

From the comparisons, both methods can achieve satisfactory attitude control effect. Traditional ADRC method attains good control performance under optimized control parameters because of its inherent disturbance rejection ability. However, ADRC cannot directly suppress the control jitters due to the controller, rather than the external disturbance oscillations, as shown in Fig. 6(b). These jitters will further cause oscillations of the inner-loop states, as the

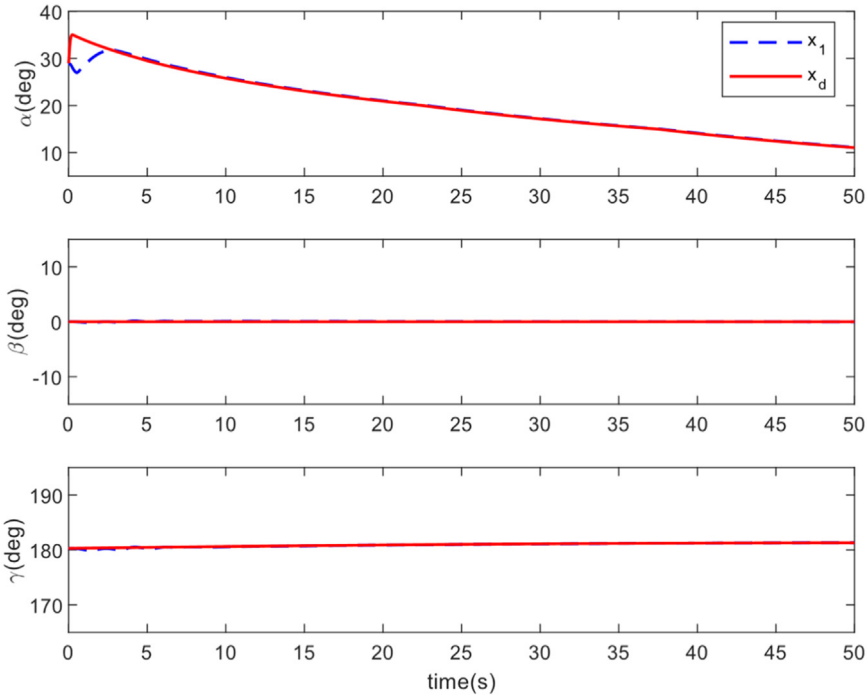

Fig. 9. Attitude angle trajectory tracking.

angular rates shown in Fig. 5(b). On the other hand, by using the proposed NNESO, the NN structure enables ESO to accurately match the disturbance characteristics. And the jitters of the controller can be suppressed effectively.

Additionally, against the multi-channel coupled control system such as the HV, the traditional ADRC decoupling control method cannot solve the coupling disturbance problem between multiple channels. From Fig. 8(c), it is evident that with ADRC method, the disturbance of rolling channel has obvious influence on other two channels. However, the problem has been significantly improved by using the proposed NNESO based ADRC method, because of the inherent multi-channel nonlinear controller design capability of neural networks.

4.4. Attitude tracking simulation

To verify the practical performance of the proposed control method, a tracking simulation of an actual trajectory is given in this paper. The same hypersonic flight vehicle dynamic model is investigated. However, we need to consider the time-varying system in attitude tracking control simulation.

The internal and external disturbances of the model are still reflected by introducing system uncertainty into the aerodynamic parameters. The additional deviations of approximately 30% for the nominal aerodynamic parameters are considered to demonstrate the attitude tracking control effect. The control parameters selected for this part of the simulation are identical to those selected in the previous part.

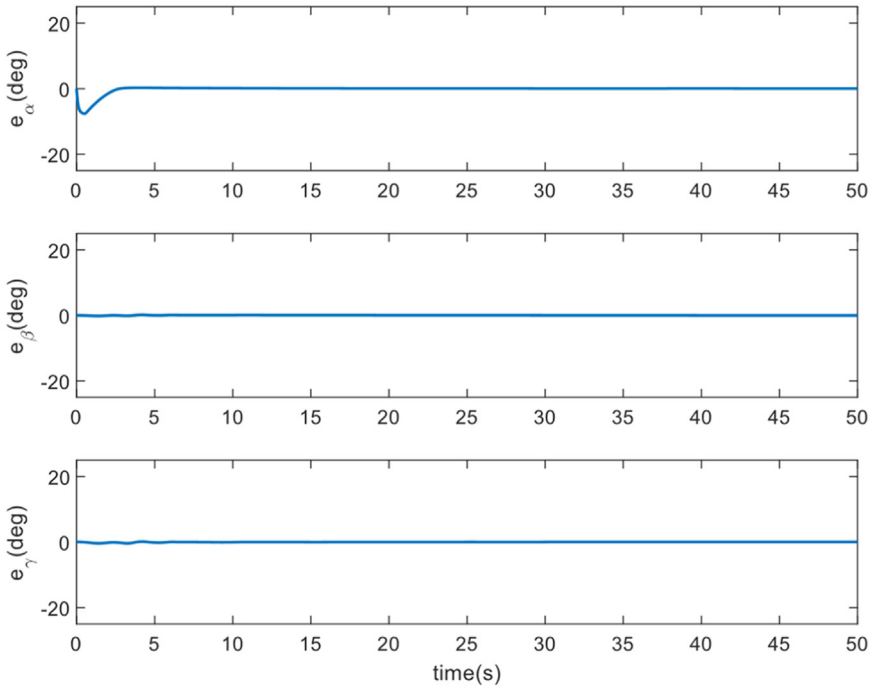

Fig. 10. Attitude angle tracking errors.

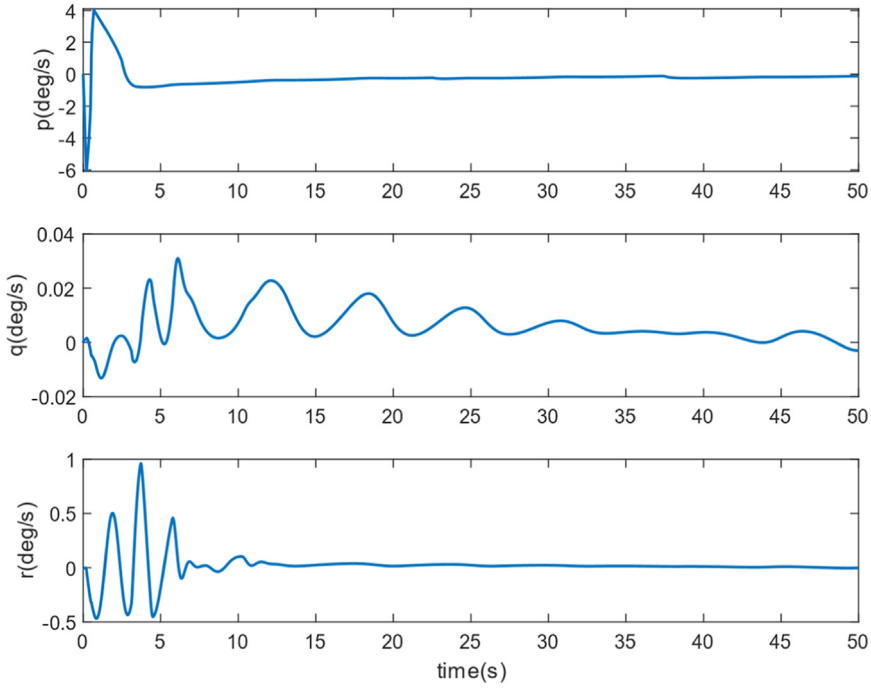

Fig. 11. Angular rates of each channel.

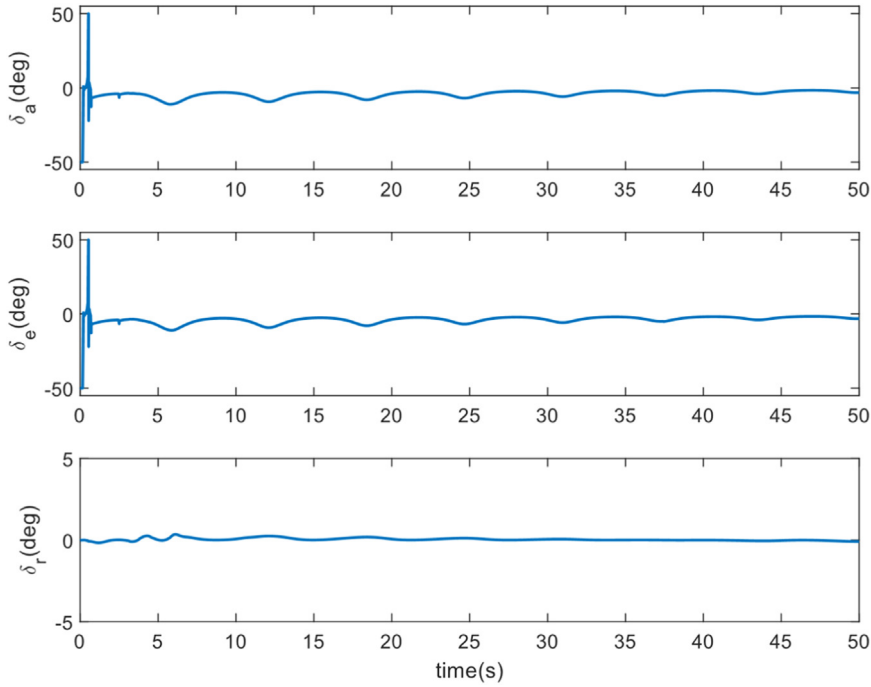

Fig. 12. Rudder angles.

The attitude trajectory of the hypersonic vehicle in the cruise segment is demonstrated. As shown in Figs. 9 and 10, the control method can quickly track the angle of attack and achieve good tracking results in the other two channels. In addition, Figs. 11 and 12 show that both the change in angular velocity and the jitter of the actual control perform well in the simulation. The angular velocity of each channel is almost smooth without burr, which shows that the neural network has a key role in disturbance recognition. Therefore, this method can be extended to the practical application of aircraft control.

5. Conclusions

In this paper, a cascade double-loop ADRC control method with a novel NNESO is designed to solve the attitude control problem of HV. The outer loop subsystem is devoted to tracking the desired attitude commands of the HV system, and the inner loop is employed to track the commands of the outer loop. According to the HV's characteristics of strong time variation and coupling, it is difficult for traditional ADRC to solve different channel disturbances of the HV. In addition, the control performance of traditional ADRC cannot be guaranteed if the parameters of ESO are not well matched with the disturbance. The RBF neural network is introduced into the ADRC combined with the ESO. The NN structure makes the observed disturbances smooth and reduces the jitter naturally in actual control. In particular, through the proposed NNESO, the hybrid disturbances among the coupling channels can be estimated integrally, which is an inherent limitation of the traditional ADRC with

the original ESO. In this way, we can directly design the controller for the hypersonic flight vehicle without decoupling.

Considering the computational cost of NN online training and its interpretability, there are few cases of direct application of the NN control method for real HV applications. This topic will be explored in our future research, where we intend to implement our method in the embedded system and to test the real-time performance of the proposed algorithm.

Declaration of Competing Interest

The author(s) declared no potential conflicts of interest with respect to the research, authorship, and/or publication of this article. Lei Liu, Yongxiong Liu, Lilin Zhou, Bo Wang, Zhongtao Cheng, Huijin Fan.

CRediT authorship contribution statement

Lei Liu: Investigation, Methodology, Project administration, Writing – review & editing. **Yongxiong Liu:** Data curation, Formal analysis, Validation. **Lilin Zhou:** Writing – original draft. **Bo Wang:** Resources, Supervision, Formal analysis. **Zhongtao Cheng:** Investigation, Conceptualization. **Huijin Fan:** Methodology, Formal analysis.

Acknowledgments

This work was supported partially by the National Natural Science Foundation of China under Grants 61873319, 61903146 and 61803162.

References

[1] D. Sziroczak, H. Smith, A review of design issues specific to hypersonic flight vehicles, Prog. Aerosp. Sci. 84 (2016) 1–28.
[2] Q. Qi, X. Bu, Adaptive dynamic programing design for the neural control of hypersonic flight vehicles, J. Frankl. Inst. 358 (16) (2021) 8169–8192.
[3] B. Chudoba, G. Coleman, A. Oza, et al., Technology and operational sensitivity assessment for hypersonic endurance flight vehicles, Aeronaut. J. 119 (1213) (2015) 365–387.
[4] B. Xu, Z.K. Shi, An overview on flight dynamics and control approaches for hypersonic vehicles, Sci. Chin. Inf. Sci. 58 (7) (2015) 1–19.
[5] H. Gao, J. Zhang, W. Tang, Offset-free trajectory tracking control for hypersonic vehicle under external disturbance and parametric uncertainty, J. Frankl. Inst. 355 (3) (2018) 997–1017.
[6] X. Zhang, Q. Zong, L. Dou, et al., Improved finite-time command filtered backstepping fault-tolerant control for flexible hypersonic vehicle, J. Frankl. Inst. 357 (13) (2020) 8543–8565.
[7] H. Zhao, Y. Liang, X. Yang, et al., Prescribed performance fine attitude control for a flexible hypersonic vehicle with unknown initial errors, Asian J. Control 20 (6) (2018) 2357–2369.
[8] B. Xu, X. Wang, Z. Shi, Robust adaptive neural control of nonminimum phase hypersonic vehicle model, IEEE Trans. Syst. Man Cybern. Syst. 51 (2) (2019) 1107–1115.
[9] Y. Cheng, B. Xu, F. Wu, et al., HOSM observer based robust adaptive hypersonic flight control using composite learning, Neurocomputing 295 (2018) 98–107.
[10] X. Yin, B. Wang, L. Liu, et al., Disturbance observer-based gain adaptation high-order sliding mode control of hypersonic vehicles, Aerosp. Sci. Technol. 89 (2019) 19–30.
[11] Y. Ding, X. Wang, Y. Bai, et al., Robust fixed-time sliding mode controller for flexible air-breathing hypersonic vehicle, ISA Trans. 90 (2019) 1–18.
[12] H. An, J. Liu, C. Wang, et al., Disturbance observer-based antiwindup control for air-breathing hypersonic vehicles, IEEE Trans. Ind. Electron. 63 (5) (2016) 3038–3049.

[13] Q. Hu, Y. Meng, C. Wang, et al., Adaptive backstepping control for air-breathing hypersonic vehicles with input nonlinearities, Aerosp. Sci. Technol. 73 (2018) 289–299.
[14] H. An, Q. Wu, C. Wang, Differentiator based full-envelope adaptive control of air-breathing hypersonic vehicles, Aerosp. Sci. Technol. 82 (2018) 312–322.
[15] S. Luo, Q. Sun, W. Wu, et al., Accurate flight path tracking control for powered parafoil aerial vehicle using ADRC-based wind feedforward compensation, Aerosp. Sci. Technol. 84 (2019) 904–915.
[16] C. Liu, G. Luo, Z. Chen, et al., A linear ADRC-based robust high-dynamic double-loop servo system for aircraft electro-mechanical actuators, Chin. J. Aeronaut. 32 (9) (2019) 2174–2187.
[17] X. Jin, T. He, X. Wu, et al., Robust adaptive neural network-based compensation control of a class of quadrotor aircrafts, J. Frankl. Inst. 357 (17) (2020) 12241–12263.
[18] D. Wu, M. Chen, H. Gong, Adaptive neural flight control for an aircraft with time-varying distributed delays, Neurocomputing 307 (2018) 130–145.
[19] Y. Huang, W. Xue, Active disturbance rejection control: methodology and theoretical analysis, ISA Trans. 53 (4) (2014) 963–976.
[20] J. Sun, Z. Pu, J. Yi, Conditional disturbance negation based active disturbance rejection control for hypersonic vehicles, Control Eng. Pract. 84 (2019) 159–171.
[21] J. Tian, S. Zhang, Y. Zhang, et al., Active disturbance rejection control based robust output feedback autopilot design for airbreathing hypersonic vehicles, ISA Trans. 74 (2018) 45–59.
[22] X. Zhang, K. Chen, W. Fu, et al., Neural network-based stochastic adaptive attitude control for generic hypersonic vehicles with full state constraints, Neurocomputing 351 (2019) 228–239.
[23] F. Albu, D. Hagiescu, L. Vladutu, et al., Neural network approaches for children's emotion recognition in intelligent learning applications, in: Proceedings of the EDULEARN 15, 7th International Conference on Education and New Learning Technologies, 2015.
[24] X. Yu, Y. Fu, P. Li, et al., Fault-tolerant aircraft control based on self-constructing fuzzy neural networks and multivariable SMC under actuator faults, IEEE Trans. Fuzzy Syst. 26 (4) (2017) 2324–2335.
[25] B. Stevens, F. Lewis, E. Johnson, Aircraft Control and Simulation: Dynamics, Controls Design, and Autonomous Systems, John Wiley & Sons, 2015.
[26] K.P. Tee, S.S. Ge, Control of fully actuated ocean surface vessels using a class of feedforward approximators, IEEE Trans. Control Syst. Technol. 14 (4) (2006) 750–756.
[27] F. Albu, A. Mateescu, J.C.M. Mota, et al., Adaptive channel equalization using neural network, in: Proceedings of the ITS'98 SBT/IEEE International Telecommunications Symposium, 2, 1998, pp. 438–441.
[28] H.G. Han, W. Lu, Y. Hou, et al., An adaptive-PSO-based self-organizing RBF neural network, IEEE Trans. Neural Netw. Learn. Syst. 29 (1) (2018) 104–117.
[29] J. Han, From PID to active disturbance rejection control, IEEE Trans. Ind. Electron. 56 (3) (2009) 900–906.
[30] S. Chen, W. Bai, Z. Chen, et al., The combination of Q-learning based tuning method and active disturbance rejection control for SISO systems with several practical factors, IFAC-PapersOnLine 53 (2) (2020) 1294–1299.
[31] J. Shaughnessy, S.Z. Pinckney, J. McMinn, et al. Hypersonic vehicle simulation model: winged-cone configuration. NASA Technical Report. 1990.
[32] S. Keshmiri, R. Colgren, M. Mirmirani, Development of an aerodynamic database for a generic hypersonic air vehicle, in: Proceedings of the AIAA Guidance, Navigation, and Control Conference and Exhibit, 2005.